University of Nebraska - Lincoln
DigitalCommons@University of Nebraska - Lincoln

Faculty Publications from Nebraska Center for Materials and Nanoscience

Materials and Nanoscience, Nebraska Center for (NCMN, formerly CMRA)

3-1-2004

Nanotube magnetism

Yucheng Sui
University of Nebraska-Lincoln, ysui2@unl.edu

Ralph Skomski
University of Nebraska-Lincoln, rskomski2@unl.edu

Kory D. Sorge
University of Nebraska-Lincoln, ksorge2@unl.edu

David J. Sellmyer
University of Nebraska-Lincoln, dsellmyer@unl.edu

Follow this and additional works at: http://digitalcommons.unl.edu/cmrafacpub

Part of the Nanoscience and Nanotechnology Commons

Sui, Yucheng; Skomski, Ralph; Sorge, Kory D.; and Sellmyer, David J., "Nanotube magnetism" (2004). *Faculty Publications from Nebraska Center for Materials and Nanoscience.* Paper 2.
http://digitalcommons.unl.edu/cmrafacpub/2

This Article is brought to you for free and open access by the Materials and Nanoscience, Nebraska Center for (NCMN, formerly CMRA) at DigitalCommons@University of Nebraska - Lincoln. It has been accepted for inclusion in Faculty Publications from Nebraska Center for Materials and Nanoscience by an authorized administrator of DigitalCommons@University of Nebraska - Lincoln.

HTML ABSTRACT + LINKS

Nanotube magnetism

Y. C. Sui, R. Skomski, K. D. Sorge, and D. J. Sellmyer[a)]
Department of Physics and Astronomy and Center for Materials Research and Analysis, University of Nebraska, Lincoln, Nebraska 68588

(Received 20 October 2003; accepted 6 January 2004)

FePt and Fe_3O_4 nanotubes are produced by hydrogen reduction in nanochannels of porous alumina templates and investigated by electron microscopy, x-ray diffraction analysis, and magnetic measurements. Loading the templates with a Fe chloride and Pt chloride mixture followed by hydrogen reduction at 560 °C leads to the formation of ferromagnetic FePt nanotubes in the alumina pores. Using a Fe nitrate solution, thermally decomposed at 250 °C and reduced in hydrogen for 2.5 h at the same temperature, yields Fe_3O_4 tubes. The length of the nanotubes is about 50 μm and their diameters range from about 150 to 220 nm, depending on the thickness of the template film and the pore diameter distribution. Reflecting the different magnetocrystalline anisotropies of the compounds, the coercivities range from 0.61 kOe for Fe_3O_4 to 20.9 kOe for FePt. The hysteresis is explained in terms of a tubular random-anisotropy model, which yields a diameter and anisotropy dependent transition from a curling-type mode (Fe_3O_4) to a localized mode (FePt). © *2004 American Institute of Physics.* [DOI: 10.1063/1.1655692]

Magnetic nanostructures are a scientifically interesting and technologically important area of research with many present and future applications in permanent magnetism, magnetic recording, and spin electronics. Recent research has led to structures such as nanodots, nanowires, and antidot structures,[1–3] and the search for novel geometries continues to be an important aspect of magnetic nanotechnology. There are many ways of producing nanostructures, such as chemical synthesis techniques[1] and template-directed growth.[4–6] An emerging area is the synthesis of tubular nanostructures, which was pioneered in inorganic chemistry.[7–9] For example, Brumlik *et al.* have produced Au microtubules by electrochemical deposition,[10] and it has been noted that the method is comparatively easy to extend to other elements, such as transition metals.[8] However, the techniques used up until now make it difficult to tune the magnetic properties of the structures. This refers, in particular, to magnetic compounds, such as hard-magnetic intermetallics and ferrimagnetic oxides used as soft and semihard magnets.

In this letter, we introduce and investigate nanotubes created by chemical deposition and hydrogen reduction in porous alumina templates. Focusing on hard-magnetic $L1_0$ FePt and on ferrimagnetic Fe_3O_4, we describe the highly efficient approach to template-directed chemical synthesis of magnetic nanotubes using hydrogen processing, elaborate upon the new physics offered by the nanotubes, and discuss potential applications.

FePt nanotubes are fabricated by wetting the substrates with alcohol and loading with a mixture of $H_2PtCl_6 \cdot 6H_2O$ and $FeCl_3 \cdot 6H_2O$ having a Fe:Pt atomic ratio of 1:1. The loaded templates are then fixed on a sample holder, with pores mounted horizontally, and placed in an oven with flowing hydrogen for 1.5 h at 560 °C. To form the ferrimagnetic Fe_3O_4 nanotubes, the substrate is similarly prepared, but the pores are loaded with 65 wt % $Fe(NO_3)_3 \cdot 9H_2O$ in alcohol solution. After mounting on a sample holder and placing in an oven, the template is first heated to 250 °C to decompose the iron nitrate before conducting hydrogen reduction at the same temperature for 2.5 h. After the nanotubes have formed, samples are etched in 0.3 M NaOH aqueous solution and the precipitates are dispersed in acetone. In both cases, templates are used to provide an array of pores with nominal diameter of 200 nm. Substrates are purchased commercially and are prepared for consistent results by preannealing in air at 600 °C for 10 min to oxidize all aluminum and remove water from the pores.[11]

Figure 1(a) shows a transmission electron microscope (TEM) image of the FePt sample taken after etching for 50 min and dispersing in acetone. The image is, actually, a composite tube, a FePt tube encased by alumina. The alumina case is retained to insure that the fragile tube, that would not be freestanding apart from the matrix, remains intact. With regard to the driving force for the formation of FePt tubes, and considering the laminar growth of Co on an Al_2O_3 substrate,[12] it is reasonable to assume a chemical bond between the interface of the FePt alloy and the inner walls of the nanochannels. Figure 1(b) shows one Fe_3O_4 nanotube released from the template. In this image, the alumina matrix is removed completely and only the magnetic nanotubes are left. Figure 1(c) shows a bundle of Fe_3O_4 nanotubes with ends pointing upward, which demonstrates clearly that magnetic nanotubes can be produced efficiently by hydrogen reduction.

Figure 2 shows x-ray diffraction (XRD) patterns of FePt and Fe_3O_4 after hydrogen reduction. The XRD data reveal that the crystal structure of Fe_3O_4 is cubic, whereas the FePt crystallizes in the tetragonal $L1_0$ structure. Both structures agree with what one expects from corresponding bulk compounds. With respect to the linewidths, the patterns are reminiscent of those of typical nanowires deposited in alumina,[4] indicating that the tubes are polycrystalline with crystallite size of a few nanometers. Polycrystalline tubes are to be

[a)]Electronic mail: dsellmyer@unl.edu

 © 2004 American Institute of Physics
Downloaded 29 Mar 2006 to 129.93.17.223. Redistribution subject to AIP license or copyright, see http://apl.aip.org/apl/copyright.jsp

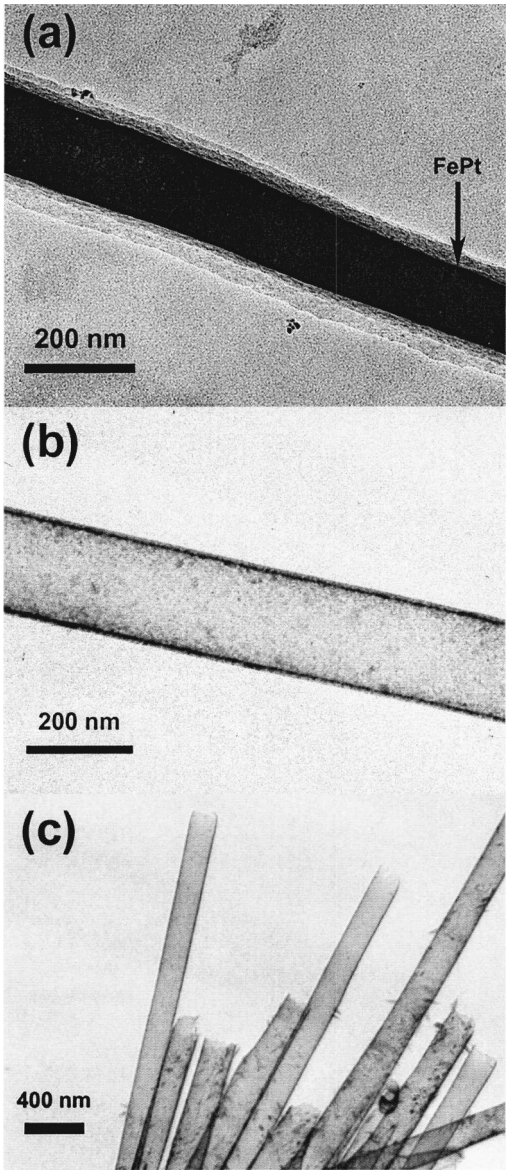

FIG. 1. TEM micrographs of the magnetic nanotubes: (a) one isolated composite nanotube of FePt surrounded by alumina, (b) one Fe_3O_4 nanotube released from the matrix, and (c) a bundle of Fe_3O_4 nanotubes.

expected, due to the precipitation from numerous random sites.

Figure 3 shows room-temperature hysteresis loops of FePt and Fe_3O_4, measured by superconducting quantum interference device (SQUID) magnetometry parallel (solid lines) and perpendicular (dashed lines) to the tube axes. While sharing some basic characteristics of magnetic hysteresis loops, the two curves exhibit two striking differences. First, the coercivity of the FePt nanotubes, about 2.09 T (20.9 kOe), is much larger than that of the Fe_3O_4 nanotubes, which is about 0.061 T (0.61 kOe). Second, the difference between the parallel and perpendicular curves is much more pronounced for the oxide tubes. Both features are related to the magnitudes of the magnetocrystalline anisotropies of the two compounds, about 6.6 MJ/m^3 for $L1_0$ FePt and -0.011 MJ/m^3 for Fe_3O_4.[2]

First, in crude approximation, the hysteresis-loop slope (or susceptibility at coercivity), $\alpha = \mathrm{d}M/\mathrm{d}H(H_c)$, is given by

$$\alpha = CH_a/M_s - D. \quad (1)$$

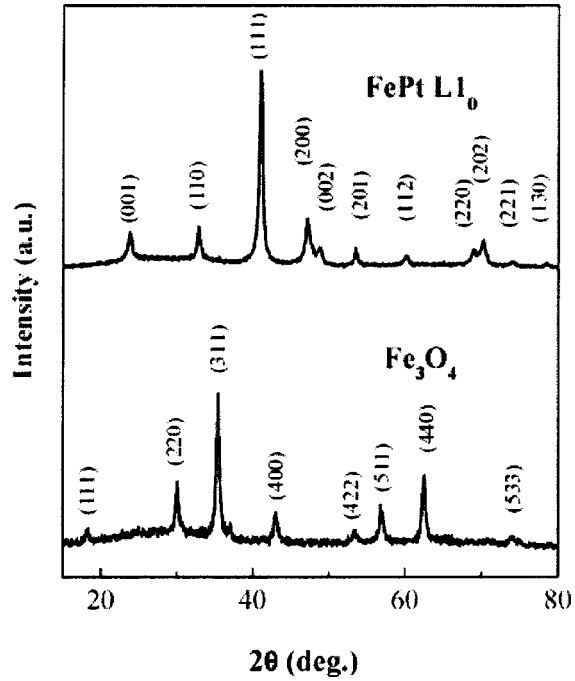

FIG. 2. X-ray diffraction patterns of FePt and Fe_3O_4 samples reduced at 560 and 250 °C, respectively.

Here M_s is the saturation magnetization, $H_a = 2K_1/M_s$ is the anisotropy field, c is a dimensionless but real-structure dependent parameter, and D is the orientation-dependent demagnetizing factor. Equation (1) predicts that the directional dependence of the hysteresis loop is least pronounced for magnetically hard materials (FePt), where $H_a \gg DM_s$. Figure 3 shows that this is indeed the case.

The huge difference in anisotropy between FePt and Fe_3O_4 leads not only to quantitative differences in H_c and the direction dependence of the loop slope it also modifies the mechanism of magnetization reversal. Figure 4 illustrates several reversal mechanisms. Magnetization curling, as shown in Figs. 4(a) and 4(b), benefits from flux closure during magnetization reversal. Coherent rotation, illustrated in Fig. 4(c), is favorable from the point of view of exchange but leads to surface poles. Like in other nanostructures, such as nanospheres and nanowires, there is a transition from coherent rotation to curling when the radius R exceeds a certain value. However, in nanotubes, this transition occurs at very small tube radius R. Using the methods outlined elsewhere[2,13,14] and evaluating the exchange energy

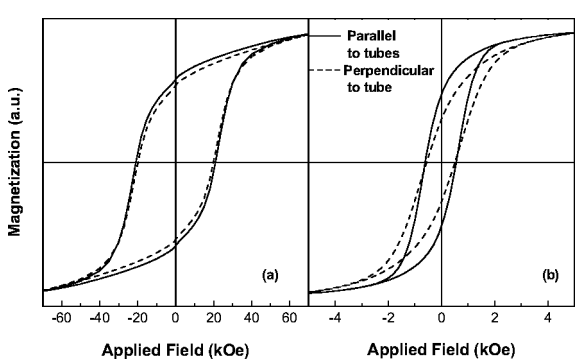

FIG. 3. Hysteresis loops measured at 300 K: (a) FePt and (b) Fe_3O_4. The external field is along and perpendicular to the tubes.

Downloaded 29 Mar 2006 to 129.93.17.223. Redistribution subject to AIP license or copyright, see http://apl.aip.org/apl/copyright.jsp

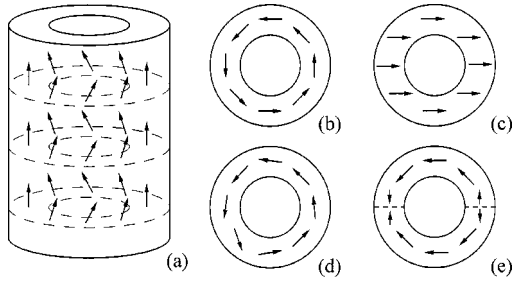

FIG. 4. Reversal modes in magnetic nanotubes: (a), (b) curling, (c) coherent rotation, (d) perturbed curling, and (e) low-lying noncurling mode. In (b) and (e), the arrows point to a small perpendicular magnetization component.

$\int A(\nabla \mathbf{M}/M_s)^2 \mathrm{d}V$ yields, for curling mode in tubes having wall thicknesses much smaller than the tube radius ($t \ll R$),

$$H_n = H_a + A/\mu_0 M_s R^2. \tag{2}$$

Here A is the exchange stiffness and M_s is the spontaneous magnetization. Comparing this expression with that for coherent rotation in long structures[2,13] shows curling occurs for radii larger than $2\ell_0$, where $\ell_0 = (A/\mu_0 M_s^2)^{1/2}$ is the exchange length of the system. For both soft-magnetic and hard-magnetic materials,[2] $2\ell_0$ is of the order 5 nm. This is smaller by a factor of 5 compared with spheres, cylinders, and other ellipsoids of revolution. The physical reason for the low exchange energy in tubes is the absence of curling-related vortices as compared to cylinders and spheres. Since the cylindrical nanotubes considered here have a radius of about 50 nm, coherent rotation can safely be ruled out.

A different issue is polycrystallinity, which may distort the curling character of the reversal mode. Figure 4(c) shows a weakly perturbed curling mode, whereas Fig. 4(d) shows a mode that has lost its curling-type flux closure. The transition between the curling mode and the localized mode in Fig. 4(d) occurs at some radius R_{rand} that depends on the magnetocrystalline anisotropy: The configuration in Fig. 4(d) is favorable from the point of anisotropy, because it has two "domains," but is unfavorable from the point of view of exchange and magnetostatics. Applying standard random-anisotropy analysis (see, e.g., Ref. 2) to the problem yields

$$R_{\mathrm{rand}} \approx \delta_B^2 t^{1/2}/a^{3/2}, \tag{3}$$

where a is the polycrystalline grain size and $\delta_B \sim (A/|K_1|)^{1/2}$ is the Bloch-wall thickness of the corresponding bulk material. Taking $a = 5$ nm, $t = 10$ nm, δ_B (FePt) $= 4$ nm, and δ_B (Fe_3O_4) $= 50$ nm yields estimates of R_{rand} (FePt) ≈ 5 nm and R_{rand} (Fe_3O_4) ≈ 700 nm. In other words, the reversal mode of the FePt nanotubes is strongly localized and has no similarity to curling, whereas the reversal in the Fe_3O_4 tubes is curling like. Note that magnetostatic self-interaction is not included in the random-anisotropy analysis leading to Eq. (3), but it can be shown that internal poles, such as those around the dashed lines in Fig. 4(e), enhance R_{rand} without invalidating the qualitative picture elaborated upon in this paragraph.

The modes shown in Fig. 4 are reversal modes, that is, they are created by a homogeneous external magnetic field. Other modes may be realized as excited modes or by applying inhomogeneous fields. For example, higher-order excitations yield spin waves with weakly localized[2] plane-wave character parallel to the tube axis but quantized in the other two directions, due to the cut-off lengths of wall thickness t and $2\pi R$. Nanotubes with very small t may lead to the direct observation of quantum-mechanical effects, such as sampling of spin-dependent electron states with quantization length of $2\pi R$.

With regard to potential applications, magnetic field sources at the nanoscale are prerequisites for making nanoelectromechanical system (NEMS) devices feasible and reliable.[15] Magnetic nanotubes are a conceivable solution to that problem. Halbach cylinders create a homogeneous cavity field which is, in general, larger than the saturation magnetization of the material. If templates with an ordered pore structure were employed, ordered arrays of magnetic nanotubes could be fabricated, and nonvolatile memory units based on the magnetization states of the nanotubes could be fabricated.[16] In addition, magnetic nanotubes also may have possible application in high-density magnetic recording,[3] biomagnetic sensors, nanomedicine, and catalysts.[16,17]

In conclusion, we have used hydrogen reduction to produce ferromagnetic nanotubes of FePt and Fe_3O_4, and investigated their structure and magnetism. A specific feature of the tubes investigated is that the magnetization reversal mode in the oxide tubes is of curling type, whereas reversal in the FePt tubes is realized by localized magnetization reversal.

This work was supported by DOE, NSF–MRSEC, AFOSR, the Center for Materials Research and Analysis, and Nebraska Research Initiative. The authors would like to thank Xingzhong Li, Jian Zhou, Kit Lee, and Joe Zhou for assistance and helpful discussions.

[1] S. Sun, C. B. Murray, D. Weller, L. Folks, and A. Moser, Science **287**, 1989 (2000).
[2] R. Skomski, J. Phys.: Condens. Matter **15**, R841 (2003).
[3] S. Khizroev, M. H. Kryder, D. Litvinov, and D. A. Thompson, Appl. Phys. Lett. **81**, 2256 (2002).
[4] D. J. Sellmyer, M. Zheng, and R. Skomski, J. Phys.: Condens. Matter **13**, R433 (2001), and references therein.
[5] Y. H. Huang, H. Okumura, G. C. Hadjipanayis, and D. Weller, J. Appl. Phys. **91**, 6869 (2002).
[6] Y. Sui, L. Yue, R. Skomski, X. Z. Li, J. Zhou, and D. J. Sellmyer, J. Appl. Phys. **93**, 7571 (2003); S. A. Chambers, T. Droubay, D. R. Jennison, and T. R. Mattsson, Science **297**, 827 (2002).
[7] M. N. Wu, Y. C. Zhu, H. G. Zheng, and Y. T. Qian, Inorg. Chem. Commun. **5**, 971 (2002).
[8] G. Tourillon, L. Pontonnier, J. P. Levy, and V. Langlais, Electrochem. Solid-State Lett. **3**, 20 (2000).
[9] J. C. Bao, C. Y. Tie, Z. Xu, Q. F. Zhou, D. Shen, and Q. Ma, Adv. Mater. (Weinheim, Ger.) **13**, 1631 (2001).
[10] C. J. Brumlik and C. R. Martin, J. Am. Chem. Soc. **113**, 3174 (1991).
[11] Y. C. Sui, B. Z. Cui, L. Martinez, R. Perez, and D. J. Sellmyer, Thin Solid Films **406**, 64 (2002).
[12] S. A. Chambers, T. Droubay, D. R. Jennison, and T. R. Mattsson, Science **297**, 827 (2002).
[13] R. Skomski and J. M. D. Coey, *Permanent Magnetism*, (Institute of Physics, Bristol, UK, 1999).
[14] R. P. Cowburn, D. K. Koltsov, A. O. Adeyeye, M. E. Welland, and D. M. Tricher, Phys. Rev. Lett. **83**, 1042 (1999).
[15] M. Zahn, J. Nanopart. Res. **3**, 73 (2001).
[16] A. S. Goldstein, M. H. Gelb, and P. J. Yager, J. Controlled Release **70**, 125 (2001).
[17] C. A. Haberzettl, Nanotechnology **13**, R9 (2002).

Downloaded 29 Mar 2006 to 129.93.17.223. Redistribution subject to AIP license or copyright, see http://apl.aip.org/apl/copyright.jsp